# Studies of Phosphonate-Containing Bismaleimide Resins. I. Synthesis and Characteristics of Model Compounds and Polyaspartimides

WEI-JYE SHU,[1,2] LI-HSIANG PERNG,[1] WEI-KUO CHIN[2]

[1] Department of Chemical Engineering, Ta-Hwa Institute of Technology, Chiung-Lin, Hsinchu 30703, Taiwan, Republic of China

[2] Department of Chemical Engineering, National Tsing Hua University, Hsinchu 30043, Taiwan, Republic of China

*Received 28 December 2000; accepted 27 April 2001*

**ABSTRACT:** Two phosphonate-containing bismaleimide (BMI) [(4,4′-bismaleimidophenyl)phosphonate] monomers with different melting temperatures and similar curing temperatures were synthesized by reacting *N*-hydroxyphenylmaleimide with two kinds of dichloride-terminated phosphonic monomers. The BMI monomers synthesized were identified with $^{1}$H-, $^{13}$C-, and $^{31}$P-nuclear magnetic resonance (NMR) spectroscopy and elemental analysis. The phosphonate-containing BMI monomers react with a free-radical initiator to prepare phosphonate-containing BMI polymers and also with various aromatic diamines to prepare a series of polyaspartimides as reactive flame retardants. The polymerization degrees of polyaspartimides depend on the alkalinity and nucleophility of diamines as chain extenders. Differential scanning calorimetry (DSC) and thermogravimetry analysis (TGA) were used to study the thermal properties of the phosphonate-containing BMI resins such as the melting temperature, curing temperature, glass transition temperature ($T_g$), and thermal resistance. All the phosphonate-containing BMI resins, except the BMI polymers, have a $T_g$ in the range of 210–256°C and show 5% weight loss temperatures ($T_{5\%}$) of 329–434 and 310–388°C in air and nitrogen atmospheres, respectively. The higher heat resistance of cured BMI resin relative to the BMI polymer is due to its higher crosslinking density. Since the recrosslinking reactions of BMI polymers and polyaspartimides occur more easily in an oxidation environment, their thermal stabilities in air are higher than are those in nitrogen gas. In addition, the thermal decomposition properties of polyaspartimides depend on the structures and compositions of both the diamine segments and the BMI segments. © 2002 John Wiley & Sons, Inc. J Appl Polym Sci 83: 1919–1933, 2002

**Key words:** phosphonate-containing bismaleimide resins; polyaspartimides; thermal resistance

## INTRODUCTION

Bismaleimide (BMI) resins can provide a higher service temperature than that of epoxy resins, while still maintaining epoxylike processing. These resins are of particular interest because of their relatively low cost, high durability, high modulus, and low flammability. As such, they have been widely used as high heat-resistance materials in the aerospace industry, in multilayer printed-circuit boards, and in surface-mounting devices as well as high-temperature adhesive agents and in many other applications. The double bond of BMI monomers, activated by the pres-

*Correspondence to:* L.-H. Perng (ceplh@ thit.edu.tw).

Contract grant sponsor: National Science Council, Taiwan; contract grant number: NSC 89-2216-E-233-001.

Journal of Applied Polymer Science, Vol. 83, 1919–1933 (2002)



DOI 10.1002/app.10019

ence of carbonyl groups, is excessively electron-depleted. Besides the self-curing of BMI, its reaction with an olefinic compound can also be performed using ENE/Diels–Alder reactions to produce the cured resin.[1,2] Also, it can form various linear polymers[3–5] through Michael addition reactions. BMI, for example, undergoes the above nucleophilic addition with thiols or hydrogen sulfide to prepare polyimidothioether[6–8] or reacts with diamine to synthesize polyaspartimide.[9,10] The molecular design of polyaspartimide is intended mainly to extend the molecule chain length of BMI, to reduce the brittleness of traditional BMI resins, to retain its thermal stability, and to exhibit better solubility and processing than those of ordinary linear polyimide. In recent years, the applications of polyaspartimide have been focused on absorbent gelling materials,[11] biodegradable materials,[11] phosphate-free detergents,[12,13] surface-active agents,[14] swelling agents of clay in nanocomposites,[15] etc.

By the introduction of phosphide, the phosphorus-containing BMI monomers can be applied as an reactive-type flame retardant to be added into resins to enhance their thermal stability and flame retardation. At present, few systematic investigations[16–19] on BMI modified by the introduction of phosphorus as a reactive flame retardant have been performed. Nevertheless, to further upgrade phosphorus-containing BMI monomers as high-performance reactants, two processing problems remain to be considered[20]: One is that when the BMI monomer is a crystalline solid with a melting point close to its curing temperature it often incurs partial curing during the preparation of a melt-blend system or incomplete reaction during the curing period. For this reason, we designed one of the phosphonate-containing BMI monomers with a relatively flexible segment in the backbone to lower its melting temperature. The other is that BMI tends to recrystallize easily from the blend system during aging. As a result, the BMI-containing blend systems often showed an inconsistent property. To improve the above drawbacks and the brittleness caused by the extensive crosslinking that occurs during polymerization, another aim of this study was to polymerize both the two phosphonate-containing BMI monomers by a free-radical initiator for studying their actual thermal properties. At the same time, a Michael addition reaction was performed between phosphonate-containing BMI monomers and different structures of diamines to synthesize various phosphonate-containing polyaspartimides for studying their molecular weights and properties.

## EXPERIMENTAL

### Materials

4-Aminophenol, maleic anhydride, and cuprous chloride were obtained from Lancaster. Triethylamine (TEA) was obtained from TEDIA. Phenyl phosphonic dichloride (PPDC) and ethyl phosphoric dichloride (EPDC) were obtained from Aldrich. 4,4′-Diaminodiphenylmethane (CA), diaminodiphenyl ether (OA), diaminodiphenyl sulfone (SA), 1,3-phenylenediamine (3A), 1,4-phenylenediamine (4A), and 2,2′-bis(4-aminophenyl)hexafluoropropane (FA) were obtained from TCI. Tetrahydrofuran (THF) was distilled after dehydration with sodium. *N,N*-Dimethylformamide (DMF) was dried by $CaH_2$ overnight. The other solvents were purified by conventional methods.

### Synthesis

#### N-*Hydroxyphenylmaleimide*[21,22]

A three-neck flask equipped with a Teflon stirrer and a thermometer is injected into nitrogen gas through a nitrogen purge tube and cooled with cold water to maintain its temperature below 15°C. This flask is first added into the solution of maleic anhydride (11 g) in 50 mL of DMF and again added dropwise into 10 g (0.0917 mol) 4-aminophenol to obtain the mixture, which is stirred about 2 h in a water bath below 15°C with a nitrogen purge so as to obtain a clear amic acid solution. Then, a mixture containing 5.5 g of phosphorus pentaoxide, 2.5 g of sulfuric acid, and 50 mL of DMF is added dropwise into this amic acid solution during a period of 1 h. The resulting mixture, after stirring at 80°C for about 6 h, is cooled and poured into 500 mL of ice water to obtain the precipitate, which is washed with deionized water and recrystallized with isopropanol and further dried in a vacuum to obtain *N*-hydroxyphenylmaleimide.

#### *Phosphonate-containing BMI Monomers*[23]

The dissolution of 0.025 mol of *N*-hydroxyphenylmaleimide, 3 mL of TEA, and 0.012 g of $Cu_2Cl_2$ in 100 mL of THF is put into the same type of flask setup as above with an ice bath and nitrogen purge at a fixed flow rate. The solution of 0.01 mol

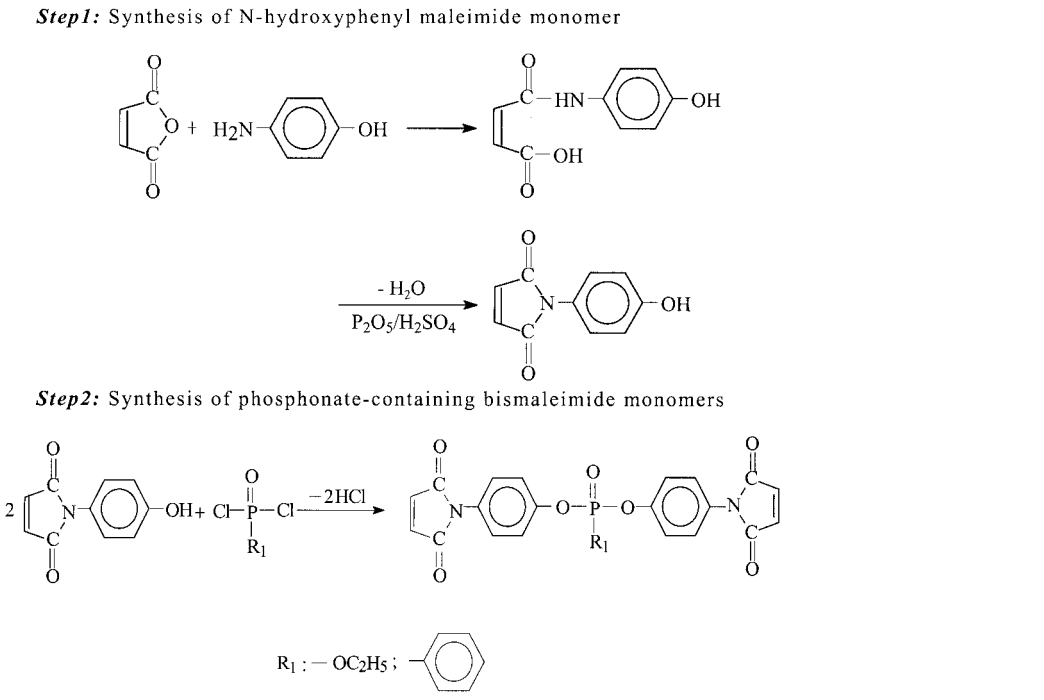


**Scheme 1**

of dichlorophosphonate (such as phenylphosphonic dichloride, PPDC) in 50 mL of THF is added gradually to the above mixture during a period of 2 h. Then, the reaction for this mixture is kept at 40°C for another 12 h. The resulting mixture is filtered to remove the precipitate of amine hydrochloride and then distilled to remove THF solvent to obtain the product, which is again dissolved in 100 mL of ethyl acetate and extracted by a 1% NaOH solution to obtain the organic layer. This organic solution, dried by anhydrous magnesium sulfate, is distilled under reduced pressure to obtain the precipitate, which is recrystallized several times with *n*-hexane and then dried in a vacuum to obtain the phosphonate-containing BMI monomer.

### *Phosphonate-containing BMI Polymers*[24]

The BMI monomer synthesized above, 2,2-azobisisobutyronitrile (AIBN; 10 mmol/L) as an initiator and toluene as a solvent are added to a flask. The free-radical polymerization of this mixture is carried out at 70°C for 10 h and then toluene is removed under reduced pressure to obtain a mixture, which is again dissolved in dichloromethane and precipitated by methyl alcohol several times to obtain the soluble BMI polymer. The resulting product after vacuum drying is weighed to obtain a yield of about 50–54%. In addition, the self-curing of the BMI monomer synthesized above is also heated at 250°C for 2 h with a nitrogen purge at a fixed flow rate to form the BMI cured resin.

### *Polyaspartimides*[25,26]

The same mol ratio of the BMI monomer (1 g) synthesized above with diamine is taken into a single-port flask with 30 mL *m*-cresol as a solvent. Another 0.l mL of acetic acid is then added into this flask which is kept in an oil bath at 130°C.

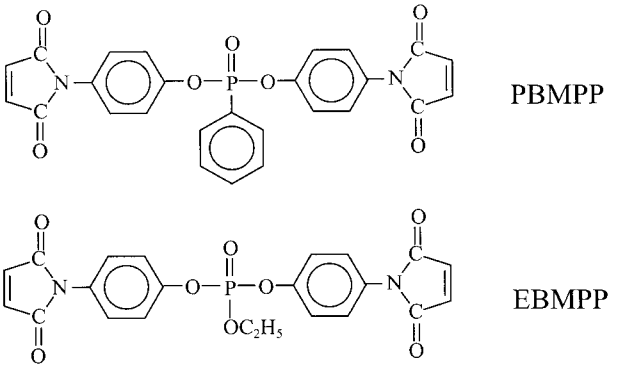


**Figure 1** Chemical structure of phosphonate-containing BMI monomers.

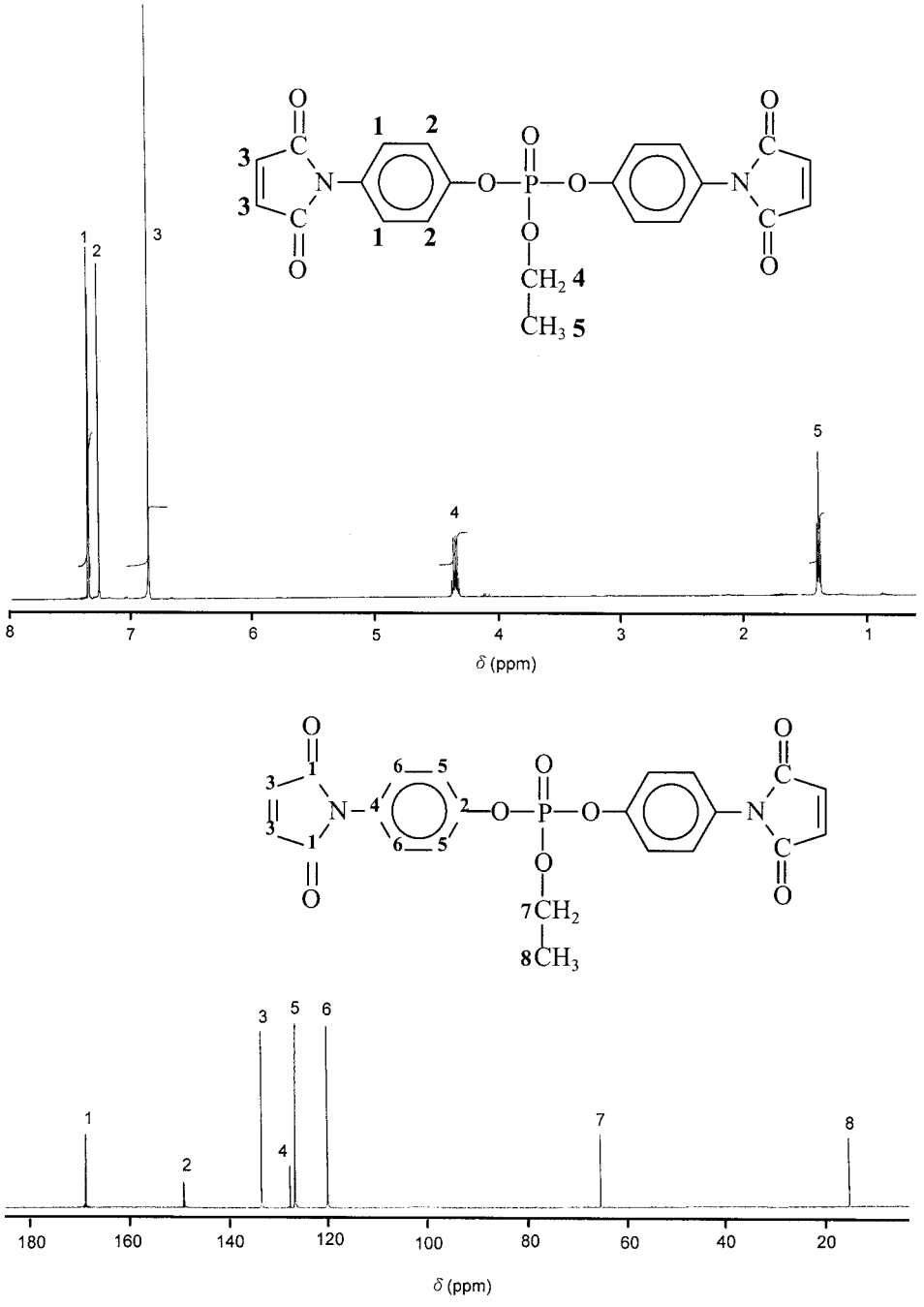


**Figure 2** $^{1}$H-NMR and $^{13}$C-NMR spectra of EBMPP.

The above reactants mixture at 130°C is further stirred about 72 h to produce a Michael addition reaction until mucus is obtained. Large amounts of methanol are poured into the above mucus to precipitate the polymer, which is then extracted several times with hot ethanol to remove the remaining solvent and nonreacting monomers to obtain polyaspartimide.

## Instrumentation

The $^{13}$C-, $^{1}$H-, and $^{31}$P-NMR spectra of all the monomers synthesized above were analyzed by a Bruker MSL NMR spectrometer. The elemental analyses (C, H, N) of these above monomers were performed with a Heraeus CHN-O Rapid element analyzer. The FTIR spectra of all the monomers

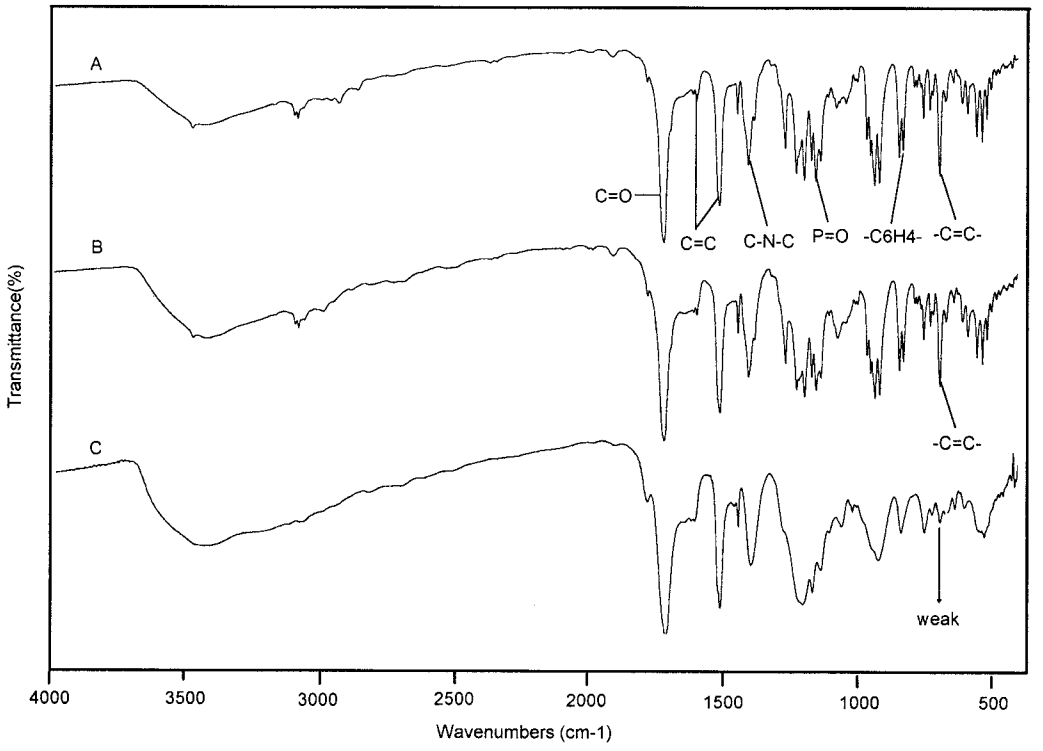


**Figure 3** FTIR spectra of PBMPP (A) monomer, (B) polymer, and (C) cured resin.

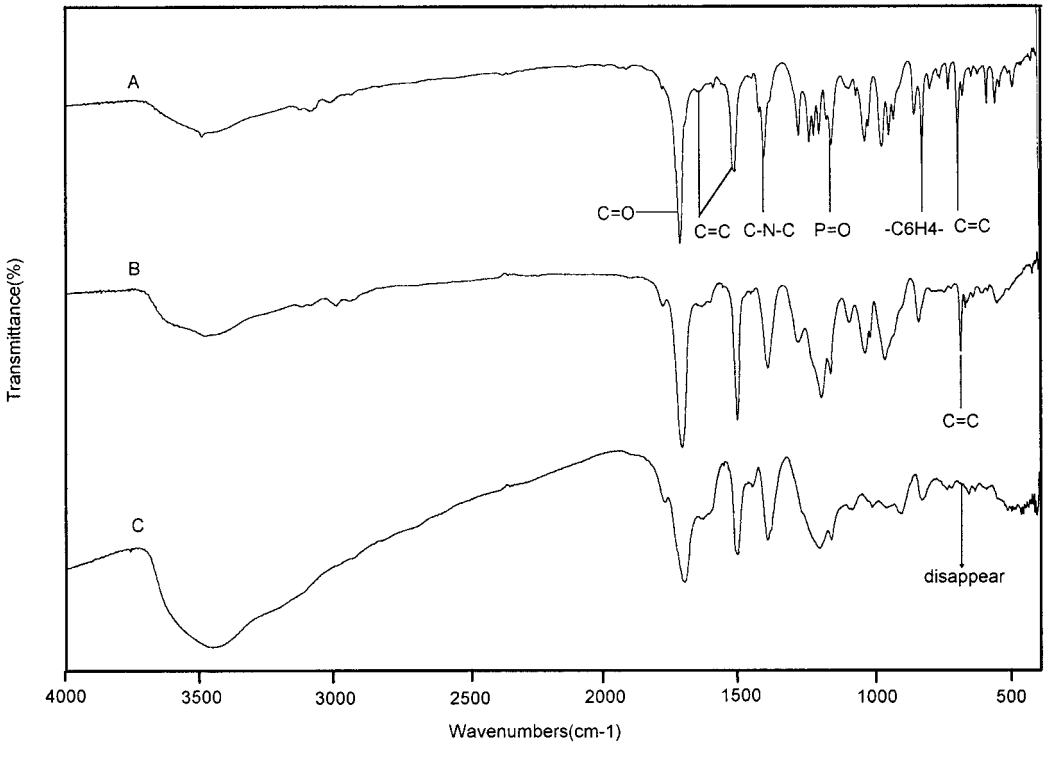


**Figure 4** FTIR spectra of EBMPP (A) monomer, (B) polymer, and (C) cured resin(C).

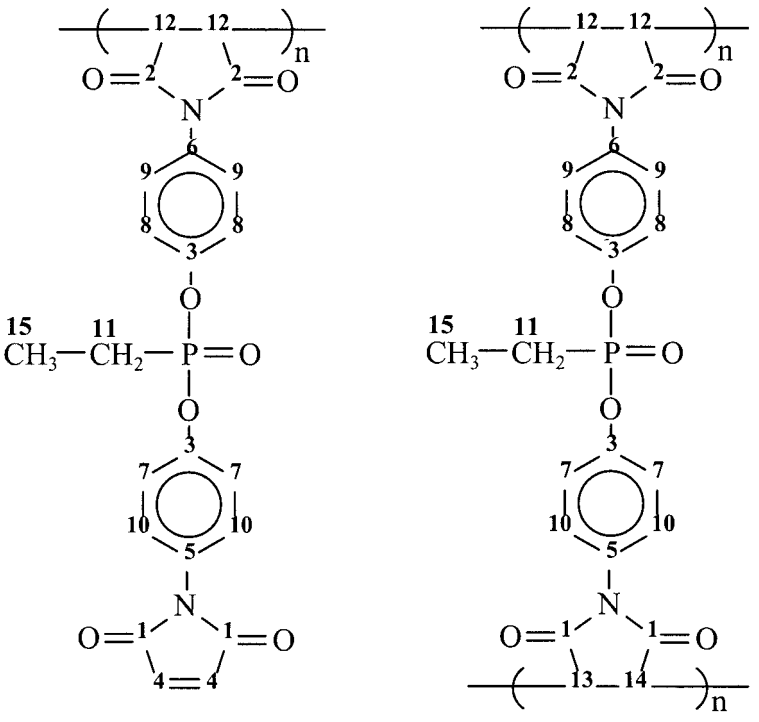

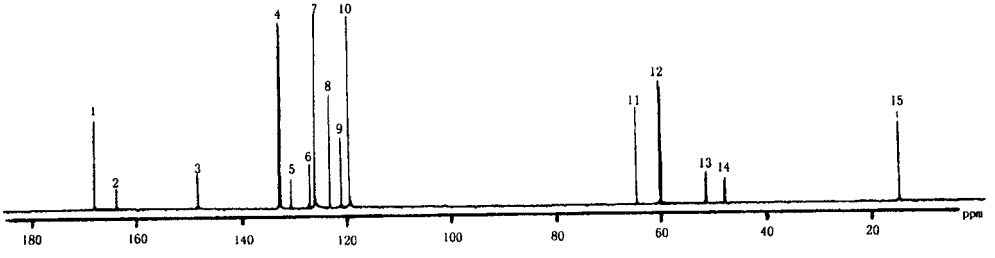


**Figure 5** $^{13}$C-NMR spectra of EBMPP polymer.

and polymers synthesized above were analyzed by a Nicolet Omnic 3 Fourier transform infrared reflection spectrophotometer. A Waters 510 gel permeation chromatography (GPC) system after using standard samples of polystyrene with a narrow molecular weight distribution calibration was then used to analyze the molecular weight distributions of the phosphonate-containing polyaspartimides with a sample concentration of 0.5 wt % in THF as an effluent flow at a flow rate of 1.0 mL/min. A Ubbelohde viscometer was used to measure the intrinsic viscosity of these soluble polymers. The melting temperature, curing temperature, and glass transition temperature of these polymers were analyzed by DSC (TA-Instruments DSC10) at a heating rate of 10°C/min in $N_2$. The thermal decomposition of the phosphonate-containing BMI resins was analyzed by TGA (TA-Instruments TGA 51) at a heating rate of 20°C/min in $N_2$ or air.

## RESULTS AND DISCUSSION

The new soluble phosphonate-containing BMI monomers were synthesized through a two-step process as shown in Scheme l. The first step is the synthesis of *N*-hydroxyphenylmaleimide via imidization,[21,22] and the second step is the synthesis of phosphonate-containing BMI monomers via a condensation reaction.[23] The monomer structures so obtained are shown in Figure 1.

### Structure Identification of BMI Monomers

#### N-*(4′-Hydroxyphenyl)maleimide (4HPMI)*

Yield 71% as orange needles; mp 185–186°C. $^1$H-NMR (*d*-chloroform), δ (ppm): 7.38 (2H,d, 2′-**H**, 6′-**H**; 7.19 (2H, d, 3′-**H**, 5′-**H**); 6.83 (2H,s, —CO—C**H**═C**H**—CO—); 3.70 (1H, 4′-O**H**). $^{13}$C-NMR (*d*-chloroform), δ (ppm): 122.5 (3′-**C**, 5′—**C**); 126.6 (1′-**C**—N—); 128.5 (2′-**C**, 6′-**C**); 134.5 (—CO—**C**H═**C**H—CO—); 150.1 (4′-**C**—OH); 168.4 (2-**C**═O).

ANAL. C, 63.1% H, 3.8%; N, 7.1%. Calcd: C, 63.5%; H, 3.7%; N, 7.4%.

#### *Phenyl(4,4′-bismaleimido phenyl)phosphonate (PBMPP)*

Yield 66% as a puce powder; mp 205°C; curing temperature 268°C. $^1$H-NMR (*d*-chloroform), δ (ppm): 7.25 (4H,s, 2′-**H**, 6′-**H**); 7.22 (4H, s, 3′-**H**, 5′-**H**); 6.81 (4H, s, —CO—C**H**═C**H**—CO—); 7.95 (2H,q, 2″-**H**, 6″-**H**); 7.52 (2H, q, 3″-**H**, 5″-**H**); 7.62 (1H, t,4″-**H**). $^{13}$C-NMR (*d*-chloroform), δ (ppm): 127.5 (3′-**C**, 5′-**C**); 129.0 (3″-**C**, 5″-**C**); 128.4 (1′-**C**—N—); 121.5 (2′-**C**, 6′-**C**); 132.4 (2″-**C**, 6″-**C**); 134.5 (—CO—**C**H═**C**H—CO—); 149.4 (4′-**C**—O—P); 169.4 (2-**C**═O); 133.8 (4″-**C**); 114.6 (1″-**C**). $^{31}$P-NMR (*d*-chloroform), δ (ppm): −7.7.

ANAL. C, 62.0%; H, 3.5%; O, 22.2%; N, 5.0%. Calcd: C, 62.4%; H, 3.4%; O, 22.4%; N, 5.6%.

#### *Ethyl(4,4′-bismaleimido phenyl)phosphonate (EBMPP)*

Yield 68% as a puce powder; mp 137°C; curing temperature 268°C. $^1$H-NMR (*d*-chloroform), δ (ppm): 7.35 (4H,s, 2′-**H**, 6′-**H** ); 7.24 (4H, s, 3′-**H**, 5′-**H**); 6.83 (4H, s, —CO—C**H**═C**H**—CO—); 4.36 (2H,q, O—C**H**$_2$—CH$_3$); 1.39 (3H,t, O—CH$_2$—C**H**$_3$). $^{13}$C-NMR (*d*-chloroform), δ (ppm): 127.5 (3′-**C**, 5′-**C**); 128.4 (1′-**C**—N—; 121.1 (2′-**C**, 6′-**C**); 152.2 (—CO—**C**H═**C**H—CO—); 149.6 (4′-**C**—O—P); 169.4 (2-**C**═O); 66.1 (O—**C**H$_2$—CH$_3$); 16.2 (O—CH$_2$—**C**H$_3$), as shown in Figure 2. $^{31}$P-NMR (*d*-chloroform), δ (ppm): −7.3.

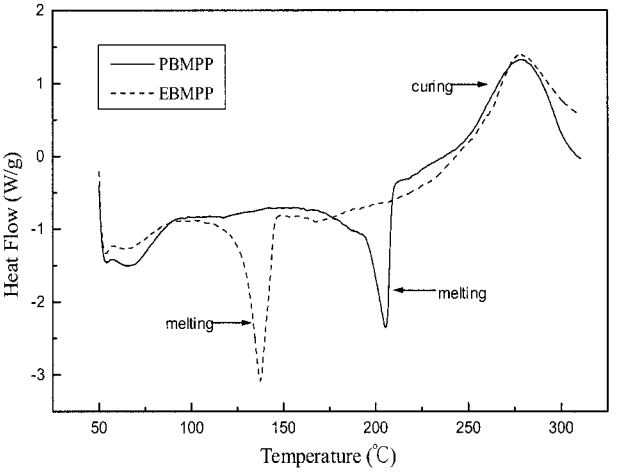


**Figure 6** DSC curves of BMI monomers in nitrogen gas.

ANAL. C, 55.8%; H, 3.7%; O, 26.8%; N, 2.8%. Calcd: C, 56.4%; H, 3.6%; O, 27.4%; N, 3.0%.

### Characteristics of BMIs

Figures 3 and 4 show FTIR spectra of the PBMPP and EBMPP monomers, polymers, and cured resins, respectively. The characteristic absorption peaks of the above BMI monomers can be seen from the FTIR spectra such as $\nu$ (cm$^{-1}$): 1713 (C═O); 1597, 1520 (C═C from benzene); 831 (disubstitution of benzene); 1400 (C—N—C); 697 (C═C from maleimide ring); 1209 (P═O), etc. The above BMI polymer can be identified from the FTIR spectra; its C═C characteristic absorption peak at position 697 cm$^{-1}$ was attenuated by the free-radical polymerization reaction but its nonpolymerized C═C bond from the maleimide ring still exists. The structure of BMI polymers can also be identified from the NMR spectra. Figure 5 shows the $^{13}$C-NMR spectrum of the EBMPP polymer. From analysis of Figure 5, there are some chemical shifts within the spectrum of this polymer including a partial crosslinking structure (—CO—**C**H—**C**H—CO—; 49.53 ppm) and nonreacted C═C double bonds (—CO—**C**H═**C**H—CO—; 134 ppm). The result of this polymer still having some unsaturated double bond, similar to the results of the FTIR analysis for this polymer, exhibits that its free-radical polymerization due to hindrance from imide and the benzene ring, or a comblike structure itself, inhibits its complete

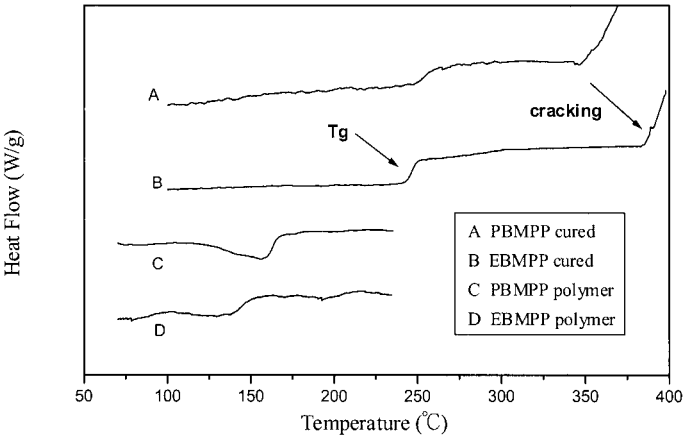


**Figure 7** DSC curves of BMI polymers and cured resins in nitrogen gas.

reaction of the double bond. In comparing the spectra of two cured BMI resins, the extent of the disappearance of the C═C characteristic absorption peak of the cured PBMPP resin is less than that of the EBMPP one, indicating that, in the same curing condition, the crosslinking degree of the former is lower than that of the latter.

The curves of two BMI monomers measured by DSC at a heating rate of 10°C/min in a nitrogen atmosphere are shown in Figure 6. There are different melting endothermic peaks around 137 and 205°C but a similar curing exothermic peak in the range of 220–320°C for these monomers. The melting point of PBMPP is higher than that of EBMPP due to the higher density of the benzene ring of the former relative to the latter and is too close to its exothermic curing temperature (220°C), leading to lower its processing window,[27] which indicates that its viscosity will increase rapidly to obstruct its evolution of blebs. In contrast, the margin between the melting temperature (137°C) and the initial polymerization temperature (220°C) of the EBMPP monomer is relatively larger, thus allowing a bigger processing window for better fusing fluidity and processing. Therefore, the self-curing of EBMPP is easier than that of PBMPP. Thus, in comparing the $T_g$ of the above polymers or cured resins in the range of 160–145 or 256–252°C, respectively, as shown in Figure 7 and given in Table I, the PBMPP's $T_g$, due to the high density of the benzene ring, is higher than that of EBMPP. When the cured BMI resins are heated in nitrogen, as seen in Figure 7, there is almost no other crosslinking reaction before they begin cracking. This result of a high crosslinking density for cured BMI resin, leading to poor fusing fluidity, indicates that few of its residual C═C bonds are reactive.

**Table I Molecular Weights and Thermal Properties of Phosphonate-containing BMI Polymers and Cured Resins**

| | | | | | $T_{5\%}$ (°C)[c] | | Char at 800°C (wt %)[c] | |
|---|---|---|---|---|---|---|---|---|
| Monomer | Yield (wt %) | $M_w$[a] | $M_n$[a] | $T_g$ (°C)[b] | Air | $N_2$ | Air | $N_2$ |
| PBMPP | 50 | 20,735 | 5344 | 160 | 295 | 305 | 31.4 | 44.2 |
| PBMPP (cured)[d] | — | — | — | 256 | 353 | 355 | 38.9 | 59.0 |
| EBMPP | 54 | 21,466 | 5881 | 145 | 304 | 300 | 40.5 | 46.6 |
| EBMPP (cured)[d] | — | — | — | 252 | 388 | 388 | 56.5 | 66.8 |

[a] Distribution of molecular weight was tested by GPC with a concentration of 0.5 wt % sample in THF.
[b] The glass transition temperature ($T_g$) was analyzed by DSC at a heating rate of 10°C/min in $N_2$.
[c] The $T_{5\%}$ and char at 800°C represents the onset temperature of 5% weight loss and yield of the solid residue, respectively, analyzed by TGA at a heating rate of 20°C/min in $N_2$ or air.
[d] Self-curing at 250°C for 2 h.

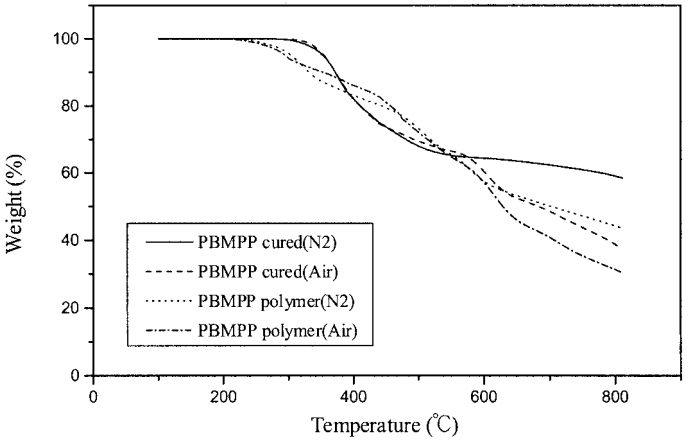


**Figure 8** TGA curves of PBMPP polymer and cured resin.

The thermal decomposition properties of the TGA curves of the two BMI polymers and the cured resins measured in nitrogen and air atmospheres, respectively, as shown in Figures 8 and 9, are listed in Table I. The decomposition for the cured BMI resin is a one-stage and two-stage process in nitrogen and air atmospheres, respectively, while for the BMI polymer, it is a two-stage and three-stage process in nitrogen and air atmospheres, respectively. These results indicate that the higher the crosslinking extent of the BMI resin is, the higher its thermal stability is. Therefore, as the BMI polymer is heated in nitrogen, its first stage should be initialized from scission of its phosphonic linkage because of its weaker bond energy. Also, its second-stage should produce random chain scission and carbonization reactions of its five-membered ring and imide chain.[23] Besides, its third-stage in air ought to produce the combustion reaction of carbonization under an oxidation environment of high temperature. Thus, the decomposition of the first two stages for this polymer in air is still similar to that in nitrogen, indicating that its dominant degradation mechanisms in the first two stages still remain unchanged in the oxidation environment. As the data given in Table I show, the $T_{5\%}$ of the PBMPP polymer (305°C) in nitrogen is higher than that of the EBMPP one (300°C), similar to the results of the $T_g$'s of these polymers. In air, the $T_{5\%}$ of the EBMPP polymer (304°C) is higher than that of the PBMPP one (295°C). The former relative to the latter, due to its higher reactivity of the residual C═C bonds in the oxidation environment, produces relatively more recrosslinking reactions during the thermal process to increase its thermal stability. In air, the decomposition of the PBMPP polymer relative to the EBMPP one, be-

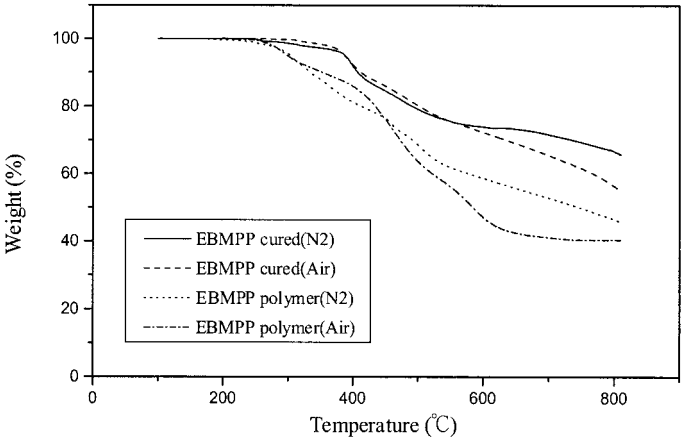


**Figure 9** TGA curves of EBMPP polymer and cured resin.

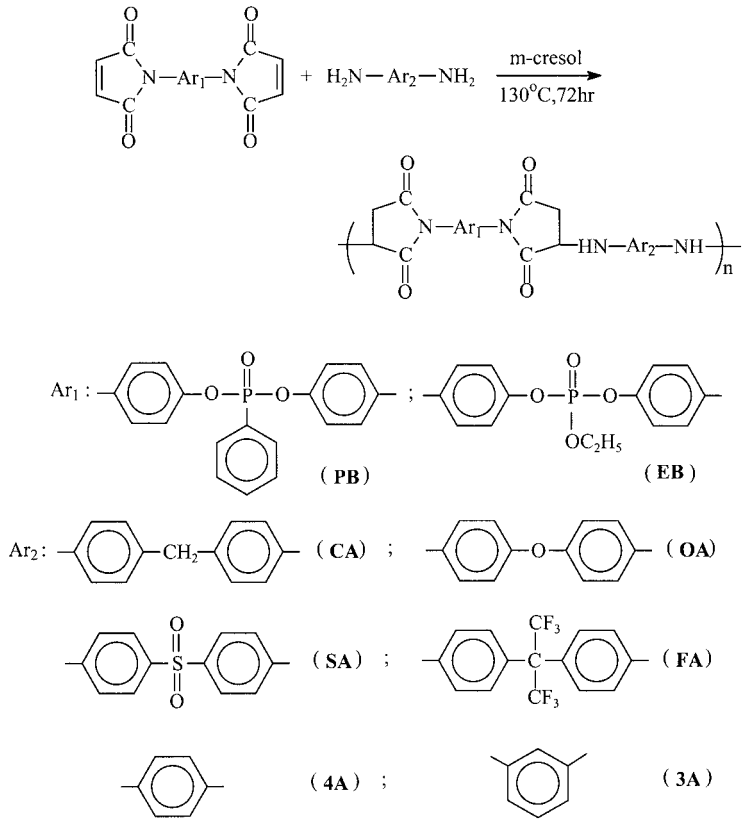


**Scheme 2**

cause of its higher phosphorus content, shows higher flame retardancy. The $T_{5\%}$ and char yields at 800°C of the EBMPP cured resin are around 388°C, 66.8% and 388°C, 56.5% in nitrogen and air atmospheres, respectively. As mentioned above, since the crosslinking density of the EBMPP cured resin is higher than that of the PBMPP one, the $T_{5\%}$ and char yield of the former are higher than those of the latter.

## Characteristics of Polyaspartimides

Polyaspartimides have been synthesized through a Michael addition reaction of the phosphonate-containing BMI monomer with various aromatic diamines,[24,25] which is illustrated in Scheme 2. Using acetic acid as a catalyst, a Michael addition reaction of the BMI monomer with various aromatic diamines is maintained for 72 h to obtain a viscous copolymer solution. After purification, the copolymer obtained above forms a powder of a dark brown color with an average yield of about 50–65% as listed in Table II. The above compounds can only be dissolved in phenol-like and amidelike polar solvents. Figure 10 shows the FTIR spectra of the PBMPP monomer before and after the addition reaction with CA and FA. It is obvious that its —NH bending is produced at the position 1640 $cm^{-1}$ and its C═C characteristic absorption peak at 697 $cm^{-1}$ is attenuated by the Michael addition reaction.

The basic properties of various polyaspartimides are given in Table II. Their intrinsic viscosity in the range of 0.5–0.65 dL/g is affected mainly by the structure of the chain extender. For example, in comparing the diphenyldiamine series polymers, the electron-withdrawing group —$SO_2$ and —$CF_3$ within their chain extenders SA and FA reduced the alkalinity and nucleophilicity of the diamines, leading to a reduction of their polymerization degree and intrinsic viscosity. Also, in comparing the phenylenediamine series polymers, because of the lower activity of the *meta* amino position of the 3A polymer relative to *para* one of the 4A one, the polymerization degree and intrinsic viscosity of the former are lower than are those of the latter. The $T_g$'s of the various polyaspartimides measured by DSC are listed in Table II. The $T_g$'s of the PBMPP (PB) series are higher than those of the EBMPP (EB) series. The results

**Table II Molecular Weights and Properties of Polyaspartimides Prepared from Reacting BMI Monomers with Various Diamines**

| Compound | Yield (wt %) | $[\eta]$[a] (dl/g) | $T_g$[b] (°C) | $M_n$[c] | $M_w$[c] | $M_w/M_n$ | DP |
|---|---|---|---|---|---|---|---|
| PB–CA | 54 | 0.604 | 228 | 7843 | 16078 | 2.05 | 11.3 |
| PB–OA | 56 | 0.651 | 226 | 6819 | 11425 | 2.09 | 9.8 |
| PB–SA | 62 | 0.550 | 242 | 6166 | 11962 | 1.94 | 8.3 |
| PB–3A | 50 | 0.535 | 245 | 6008 | 14720 | 2.45 | 9.9 |
| PB–4A | 65 | 0.630 | 252 | 6846 | 14514 | 2.12 | 11.3 |
| PB–FA | 48 | 0.509 | 235 | 6558 | 14100 | 2.15 | 8.0 |
| EB–CA | 58 | 0.585 | 215 | 7256 | 14657 | 2.02 | 10.9 |
| EB–OA | 55 | 0.565 | 210 | 6237 | 13160 | 2.11 | 9.4 |
| EB–SA | 60 | 0.522 | 225 | 6613 | 13292 | 2.01 | 9.3 |
| EB–3A | 52 | 0.526 | 235 | 5916 | 14080 | 2.38 | 10.3 |
| EB–4A | 62 | 0.639 | 242 | 6748 | 14981 | 2.22 | 11.8 |
| EB–FA | 50 | 0.524 | 223 | 6073 | 13664 | 2.25 | 7.7 |

[a] Intrinsic viscosities measured in DMF at 30°C.
[b] The glass transition temperature was analyzed by DSC at a heating rate of 10°C/min in $N_2$.
[c] Distribution of molecular weight is tested by GPC with a concentration of a 0.5 wt % sample in THF as a solvent.

are similar to those of the BMI-cured resins and polymers. For the above two series polymers, their $T_g$'s for the same BMI segment are apparently decided by the mobility or chain flexibility of their diamine segments in the order of 4A3ASAFAOACA.

Figures 11 and 12 show the TGA curves of the PB series polyaspartimides measured in nitrogen and air, respectively, while their thermal decomposition properties are listed in Table III. As seen in Figures l1 and 12, except for the FA segment polyaspartimide in air, thermal decomposition processes for the PB series polyaspartimides are similar to those for the BMI polymers, which proceed through two-stage and three-stage cracking under nitrogen and air atmospheres, respectively. Therefore, the decomposition of the first stage for polyaspartimides in a nitrogen atmosphere should be first initialized by scission of the phosphonate or HN—C (secondary amine) linkage with the weaker bonding, and then after the first stage, it is similar to those for the BMI polymers. In an air atmosphere, the decomposition of first two stages for polyaspartimides is still similar to those in nitrogen. But in comparing the $T_{5\%}$ in nitrogen and in air atmospheres, respectively, as listed in Table III, their reaction of a residue double bond with an amine-terminated chain or

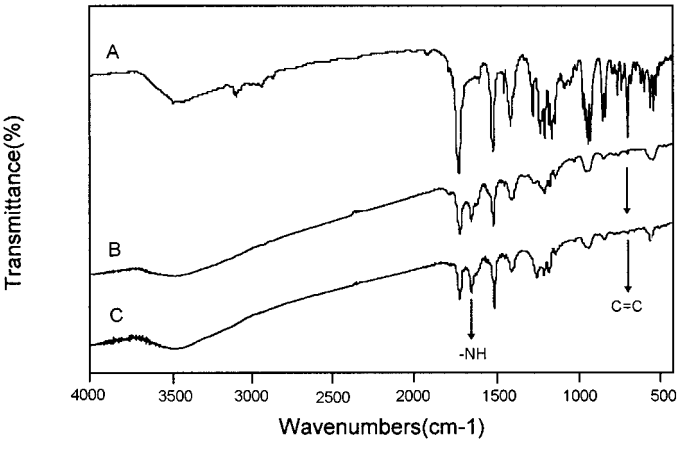


**Figure 10** FTIR spectra of (A) PBMPP monomer, (B) PB–CA polyaspartimide, and (C) PB–FA polyaspartimide.

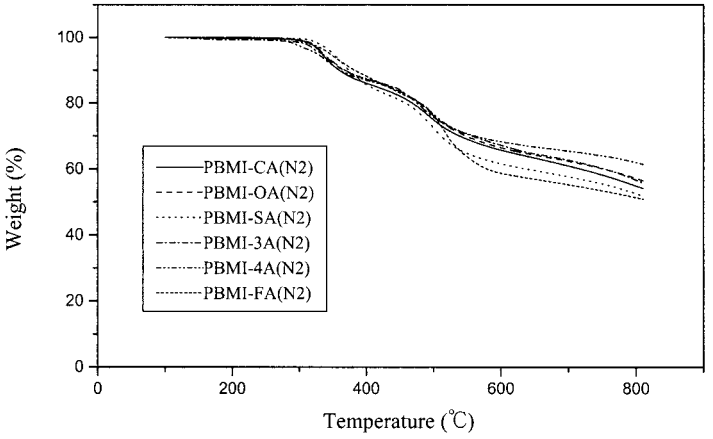


**Figure 11** TGA curves of PBMPP series polyaspartimides in nitrogen gas.

themselves during the first two stages should be catalyzed by the oxidation environment to produce the repolymerization reaction, leading to an increase in their thermal stability. These results also indicate that the decomposition and repolymerization of the first two stages can proceed simultaneously in the oxidation environment. Only in the third stage is their decomposition at high temperature governed mainly by thermal oxidation. In addition, the $T_{5\%}$ values of these above polymers are also affected by the thermal stability of the diamines. For example, because of the higher thermal stability of $SO_2$ and $CF_3$ groups of SA- and FA-segment polymers relative to the others, the $T_{5\%}$'s of the former two reach 350 and 346°C in a nitrogen atmosphere and 357 and 376°C in an air atmosphere, respectively, which are higher than those of the latter. The carbonized char yield at 800°C for the 4A-segment polyaspartimide due to a higher phosphorus content is the highest of all the others and is about 62.0 and 44.6% in nitrogen and air atmospheres, respectively, while for the FA-segment polyaspartimide, it is the lowest of all the others because of both its lower phosphorus content and larger proportion fluorine release and is about 51.3& and 7.3% in nitrogen and air atmospheres, respectively. The results of the FA-segment polyaspartimide decomposed in air to form a lower char yield of a solid residue relative to the others indicate that the fluorine content inhibits its carbonization reaction in the oxidation environment[28] and rapidly reduces its char yield. In addition, the introduction of FA into this polymer can apparently increase its thermal stability in air, leading a change in its decomposition process from three stages to two stages.

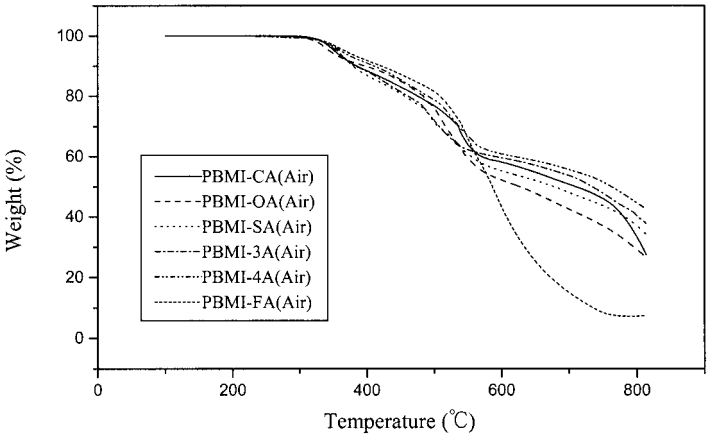


**Figure 12** TGA curves of PBMPP series polyaspartimides in air.

**Table III Thermal Decomposition Properties of Polyaspartimides Prepared from Reacting BMI Monomers with Various Diamines**

| Monomer Compositions | $P$ (wt %)[a] | $F$ (wt %)[a] | $T_{5\%}$ (°C)[b] | | Char at 800°C (wt %)[b] | |
|---|---|---|---|---|---|---|
| | | | Air | $N_2$ | Air | $N_2$ |
| PB–CA | 4.4 | 0 | 351 | 333 | 33.3 | 54.9 |
| PB–OA | 4.4 | 0 | 344 | 336 | 29.2 | 57.2 |
| PB–SA | 4.2 | 0 | 357 | 350 | 37.0 | 52.6 |
| PB–3A | 5.1 | 0 | 356 | 321 | 40.4 | 56.7 |
| PB–4A | 5.1 | 0 | 361 | 327 | 44.6 | 62.0 |
| PB–FA | 3.8 | 13.9 | 367 | 346 | 7.3 | 51.3 |
| EB–CA | 4.7 | 0 | 345 | 310 | 12.6 | 41.1 |
| EB–OA | 4.7 | 0 | 367 | 323 | 12.1 | 55.5 |
| EB–SA | 4.3 | 0 | 329 | 326 | 5.9 | 41.8 |
| EB–3A | 5.4 | 0 | 356 | 316 | 16.3 | 49.8 |
| EB–4A | 5.4 | 0 | 373 | 320 | 18.5 | 53.5 |
| EB–FA | 3.9 | 14.5 | 434 | 337 | 14.7 | 39.2 |

[a] The theoretical calculation weight ratio of the P/F composition in polyaspartimide.
[b] The thermal decomposition properties were analyzed by TGA at a heating rate of 20°C in $N_2$ or air.

The thermal decomposition properties of the EB series polyaspartimides measured by TGA in nitrogen and air atmospheres, respectively, as shown in Figures 13 and 14, are listed in Table III. In comparing the decomposition of the EB series with the PB series polyaspartimides in nitrogen or in air, the thermal stability and the char yield of the former are lower than those of the latter. A higher phenyl density for the PB series relative to the EB series polyaspartimides can enhance, simultaneously, their thermal stability and char yield of carbonization, which is dissimilar to the results of the BMI self-cured resins and polymers. Therefore, thermal decomposition for these polyaspartimides apparently depends on their structure and composition of diamine segments and BMI segments. Thus, the $T_{5\%}$'s of the EB series polyaspartimides are in the range of 310–337 and 329–434°C in nitrogen and air atmospheres, respectively. In comparing the above results of the two polyaspartimides series as seen in Figures 13 and 14 and Figures 11 and 12, especially in air, the decomposition processes of the former are evidently different from those of the latter. As shown in Figure 15, except for the SA one, there are obvious recrosslinking reactions within the EB series polyaspartimides between 250 and 350°C in air, indicating that their residue

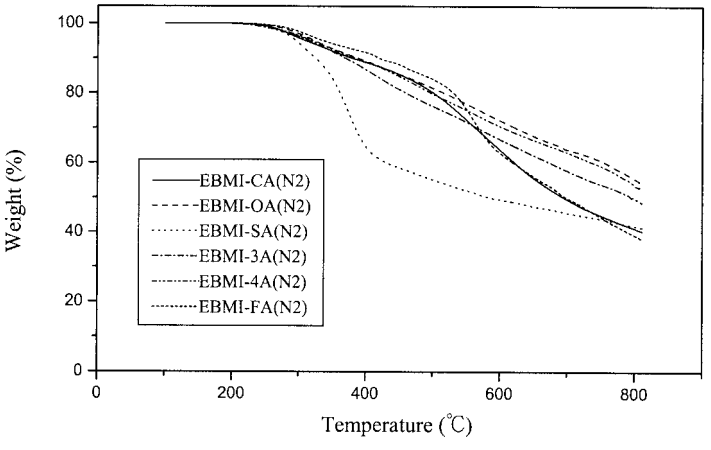


**Figure 13** TGA curves of EBMPP series polyaspartimides in nitrogen gas.

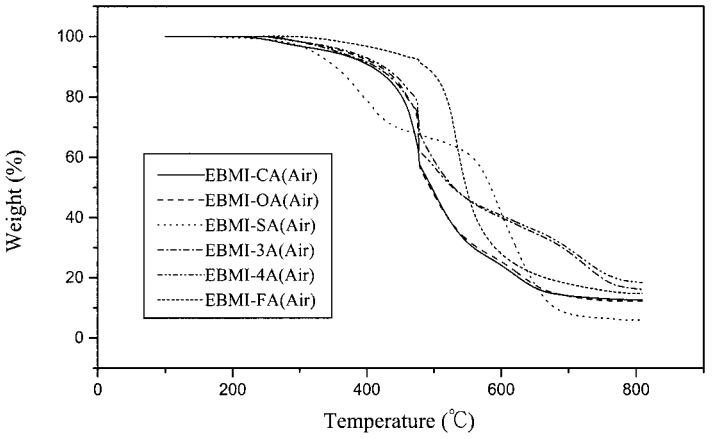


**Figure 14** TGA curves of EBMPP series polyaspartimides in air.

double bond is easily catalyzed by the oxidation environment to produce the above reaction. These phenomena indicate that the former more easily produce the recrosslinking reaction of the double bond from the maleimide ring than do the latter. Then, the decomposition for the SA-segment polyaspartimides, whether in the EB series or the PB series, may decompose more easily and release large amounts of $SO_2$ gas, leading to inhibit its recrosslinking reaction catalyzed by oxidation. These results of char yields at 800°C for the EB series polyaspartimides around 39.2–55.5 and 5.9–18.5% in nitrogen and air atmospheres, respectively, indicate that they are more easily oxidized than is the PB series These facts confirm that the thermal stability and flame retardancy of polyaspartimides are affected mainly by their structure and compositions of amine segments and BMI segments.

## CONCLUSIONS

The synthesis of two phosphonate-containing BMI monomers by a two-step process was performed by imide and condensation reactions. The temperature margin between the fusing temperature and the initial self-curing temperature for the EBMPP monomer is relatively larger than that for PBMPP, indicating that the former produces a larger processing window relative to the latter. This result makes the higher self-curing degree of the former relative to the latter increase its thermal stability and flame retardancy. The $T_g$ of the PBMPP-cured resin with a high phenyl density is higher than that of the EBMPP one. The EBMPP polymer relative to the PBMPP one, as catalyzed by oxygen in air, can produce more easily the recrosslinking reaction to promote its thermal stability and flame retardancy. Besides,

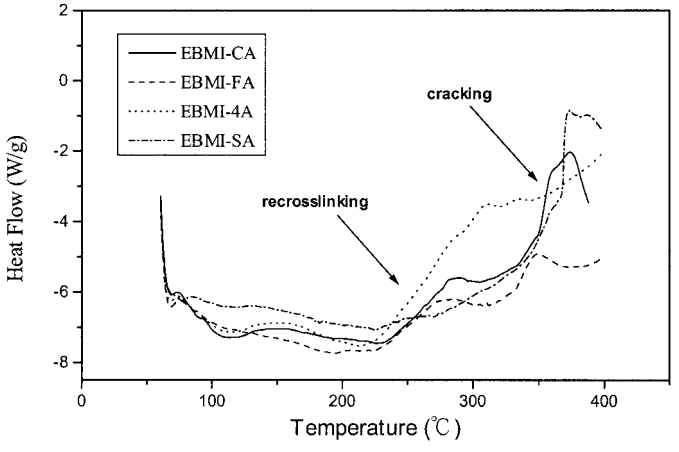


**Figure 15** DSC curves of EBMPP series polyaspartimides in air.

because of the higher phosphorus content of the EBMPP relative to the PBMPP, the char yield of the former, whether in a soluble polymer or a cured resin, is higher than that of the latter. The phosphonate-containing polyaspartimides were synthesized by the phosphonate-containing BMI monomers reacting with diamines as a chain-extender agent. The polymerization degree of the polyaspartimides synthesized depends on the alkalinity and nucleophility of the diamines. Besides, the thermal stability and flame retardancy of the PB series due to the high phenyl density are higher than are those of the EB series. The thermal decomposition of polyaspartimides, except for the SA segment, depends on their recrosslinking reactions catalyzed by the oxidization environment. Especially, the increased degree of the thermal stability for the EB series is apparently higher than that for the PB series. The properties of the phosphonate-containing polyaspartimides or BMI polymers, as above, depend on their structures and compositions, which can allow them to be used as a superior flame retardant.

The authors would like to acknowledge the financial support for this research from the National Science Council, Taiwan, under Contact NSC 89-2216-E-233-001.

## REFERENCES

1. Ottenbrite, R. M.; Smith, J. G.; Yoshimatsu, A. Polym Prepr 1987, 28, 280.
2. Ottenbrite, R. M.; Smith, J. G. Polym Prepr 1989, 30, 169.
3. Harris, F. W.; Norris, S. O. J Polym Sci Polym Chem 1973, 11, 2143.
4. Ryntz, R. A.; Kohl, R. T. Polym Prepr 1983, 24, 322.
5. Sun, K. K. Macromolecules 1987, 20, 726.
6. Crivello, J. V. J Polym Sci Polym Chem Ed 1976, 14,159.
7. White, J. E.; Scaia, M. D.; Snider, D. A. Polym Prepr 1985, 26, 132.
8. Koelling, A.; Sirendran, G.; James, W. J. J Appl Polym Sci 1992, 45, 669.
9. Crivello, J. V. J Polym Sci Chem Ed 1973, 111, 1185.
10. Varma, I. K.; Guptam, A. K.; Sangita; J Polym Lett Ed 1982, 20, 621.
11. Sikes, S. C. PCT Int. Appl. WO9 728 219, Al,7, P92, 1997.
12. Matthias, K.; Gunnar, S.; Richard, B. Ger. Offen. DE4 327 494, Al, 23, P8, 1995.
13. Matthias, K.; Gunnar, S.; Richard, B. Ger. Offen. DE19 511 859, Al, 2, P5, 1996.
14. Matthias, K.; Gunnar, S.; Richard, B. Ger. Offen. DE4 444 975, Al, 20, P4, 1996.
15. Matthias, K.; Gunnar, S.; Richard, B. Ger. Offen. DE4 300 020, Al, 7, P13, 1994.
16. Martinez-Nunez, M. F.; Sekharipurum, V. N.; McGrath, J. E. Polym Prep 1994, 35, 709.
17. Varma, I. K.; Fohlen, G. M.; Parker, J. A. J Polym Sci Polym Chem Ed 1983, 21, 2017.
18. Varma, I. K.; Fohlen, G. M.; Parker, J. A. J Macromol Sci Chem A 1983, 19, 209.
19. Wang, C. S.; Lin, C. H. Polymer 1999, 40, 5665.
20. Lin, K. F.; Lin, J. S. J Appl Polym Sci 1994, 51, 513.
21. Kawahara, H.; Maikuma, T. JK 7 435 379.
22. Oba, M.; Kawamata, M.; Tsuboi, H.; Koga, S. JK 7 966 671.
23. Liu, Y. L.; Hsiue, G. H.; Chiu, Y. S.; Jeng, R. J.; Ma, C. J Appl Polym Sci 1996, 59, 1619.
24. Matsumoto, A.; Hasegawa, K.; Fukuda, A.; Otsuki, K. J Appl Polym Sci 1991, 43, 365.
25. Crivello, J. V. J Polym Sci Polym Chem Ed 1973, 11, 1185.
26. White, J. E.; Scaia, M. D.; Snider, D. A. J Appl Polym Sci 1984, 29, 891.
27. Hwang, H. J.; Wang, C. S. J Appl Polym Sci 1998, 68, 1199.
28. Gupta, B.; Scherer, G. G. Angew Makromol Chem 1993, 210, 151.